

Parton Showering with Higher Logarithmic Accuracy for Soft Emissions

Silvia Ferrario Ravasio¹,¹ Keith Hamilton²,² Alexander Karlberg¹,¹ Gavin P. Salam,^{3,4}
 Ludovic Scyboz³,³ and Gregory Soyez^{1,5}^{1,5}

¹*CERN, Theoretical Physics Department, CH-1211 Geneva 23, Switzerland*

²*Department of Physics and Astronomy, University College London, London WC1E 6BT, United Kingdom*

³*Rudolf Peierls Centre for Theoretical Physics, Clarendon Laboratory, Parks Road, Oxford OX1 3PU, United Kingdom*

⁴*All Souls College, Oxford OX1 4AL, United Kingdom*

⁵*IPhT, Université Paris-Saclay, CNRS UMR 3681, CEA Saclay, F-91191 Gif-sur-Yvette, France*

 (Received 4 August 2023; revised 13 September 2023; accepted 14 September 2023; published 18 October 2023)

The accuracy of parton-shower simulations is often a limiting factor in the interpretation of data from high-energy colliders. We present the first formulation of parton showers with accuracy 1 order beyond state-of-the-art next-to-leading logarithms, for classes of observables that are dominantly sensitive to low-energy (soft) emissions, specifically nonglobal observables and subjet multiplicities. This represents a major step toward general next-to-next-to-leading logarithmic accuracy for parton showers.

DOI: [10.1103/PhysRevLett.131.161906](https://doi.org/10.1103/PhysRevLett.131.161906)

Parton showers simulate the repeated branching of quarks and gluons (partons) from a high momentum scale down to the nonperturbative scale of quantum chromodynamics (QCD). They are one of the core components of the general-purpose Monte Carlo event-simulation programs that are used in almost every experimental and phenomenological study involving high-energy particle colliders such as CERN’s Large Hadron Collider (LHC). Parton-shower accuracy is critical at colliders, both because it limits the interpretation of data and because of the increasing importance of showers in training powerful machine-learning-based data-analysis methods.

In the past few years it has become clear that it is instructive to relate the question of parton-shower accuracy to a shower’s ability to reproduce results from the field of resummation, which sums dominant (logarithmically enhanced) terms in perturbation theory to all orders in the strong coupling, α_s . Given a logarithm L of some large ratio of momentum scales, resummation accounts for terms $\alpha_s^n L^{n+1-p}$, N^p LL in a leading-logarithmic counting for $L \sim 1/\alpha_s$, or $\alpha_s^n L^{2n-p}$, N^p DL in a double-logarithmic counting, for $L \sim 1/\sqrt{\alpha_s}$.

Several groups have recently proposed parton showers designed to achieve next-to-leading logarithmic (NLL) and next-to-double logarithmic (NDL) accuracy for varying sets of observables [1–10]. A core underlying requirement is the condition that a shower should accurately reproduce the tree-level matrix elements for configurations with any

number of low-energy (“soft”) and/or collinear particles, as long as these particles are well separated in logarithmic phase space [2,11,12].

In this Letter, we shall demonstrate a first major step toward the next order in resummation in a full parton shower, concentrating on the sector of phase space involving soft partons. This sector is connected with two important aspects of LHC simulations, namely the total number of particles produced, and the presence of soft QCD radiation around leptons and photons (“isolation”), which is critical in their experimental identification in a wide range of LHC analyses. The corresponding areas of resummation theory, for subjet multiplicity [13–15] and so-called nonglobal logarithms [16–42], have seen extensive recent developments towards higher accuracy in their own right, with several groups working either on next-to-next-to-double logarithmic (NNDL) accuracy, $\alpha_s^n L^{2n-2}$, for multiplicity [43,44] or next-to-single logarithmic (NSL) accuracy, $\alpha_s^n L^{n-1}$, for nonglobal logarithms [45–48].

To achieve NSL or NNDL accuracy for soft-dominated observables, a crucial new ingredient is that the shower should obtain the correct matrix element even when there are pairs of soft particles that are commensurate in energy and in angle with respect to their emitter. Several groups have worked on incorporating higher-order soft or collinear matrix elements into parton showers [49–58]. Our approach will be distinct in two respects: firstly, that it is in the context of a full shower that is already NLL accurate, which is crucial to ensure that the correctness of any higher-order matrix element is not broken by recoil effects from subsequent shower emissions; and secondly in that we will be able to demonstrate the logarithmic accuracy for concrete observables through comparisons to known resummations.

Published by the American Physical Society under the terms of the Creative Commons Attribution 4.0 International license. Further distribution of this work must maintain attribution to the author(s) and the published article’s title, journal citation, and DOI. Funded by SCOAP³.

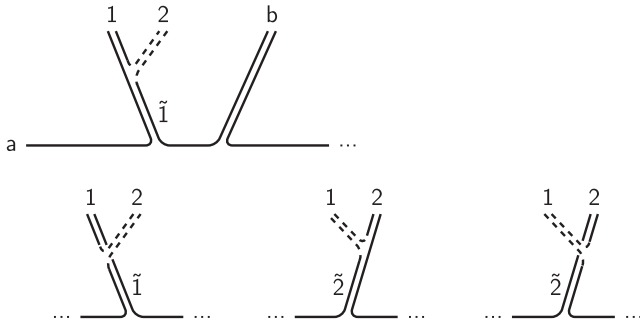


FIG. 1. Top: one shower history that produced a proximate $\{1, 2\}$ soft pair. Bottom: other histories that could have led to the same configuration of momenta, also taken into account in correcting the branching. The dashed parton is emitted second in the showering history.

We will work in the context of the ‘‘PanGlobal’’ family of parton showers, concentrating on the final-state case [2]. As is common for parton showers, it organizes particles into color dipoles [59], a picture based on the limit of a large number of colors N_c . Such showers iterate $2 \rightarrow 3$ splitting of color dipoles, each splitting thus adding one particle to the ensemble, and typically breaking the original dipole into two dipoles. The splittings are performed sequentially in some ordering variable, v , for example in decreasing transverse momentum k_t . Given a dipole composed of particles with momenta \tilde{p}_i and \tilde{p}_j , the basic kinematic map for producing a new particle k is

$$\tilde{p}_k = a_k \tilde{p}_i + b_k \tilde{p}_j + k_\perp, \quad (1a)$$

$$\tilde{p}_i = (1 - a_k) \tilde{p}_i, \quad (1b)$$

$$\tilde{p}_j = (1 - b_k) \tilde{p}_j. \quad (1c)$$

followed by a readjustment involving all particles so as to conserve momentum; see Supplemental Material [60], Sec. I. For the original PanGlobal NLL shower, the splitting probability was given by

$$\frac{d\mathcal{P}_{n \rightarrow n+1}}{d \ln v} = \sum_{\{i,j\} \in \text{dip}} \int d\tilde{\eta} \frac{d\phi \alpha_s(k_t)}{2\pi \pi} \left(1 + \frac{\alpha_s(k_t) K_{\text{CMW}}}{2\pi} \right) \times [f(\tilde{\eta}) a_k P_{\tilde{\tau} \rightarrow ik}(a_k) + f(-\tilde{\eta}) b_k P_{\tilde{\tau} \rightarrow jk}(b_k)]. \quad (2)$$

Here, $P_{\tilde{\tau} \rightarrow ik}(a_k)$ is a leading-order QCD splitting function, $\tilde{\eta} = \frac{1}{2} \ln a_k/b_k + \text{const.}$, with the constant arranged so that $\tilde{\eta} = 0$ when the emission bisects the dipole in the event center-of-mass frame, and $f(\tilde{\eta}) = 1/(1 + e^{-2\tilde{\eta}})$ is a partitioning function. Additionally, the $\overline{\text{MS}}$ coupling, $\alpha_s(k_t)$, uses at least 2-loop running, and $K_{\text{CMW}} = (67/18 - \pi^2/6)C_A - 5/9n_f$ [61].

In moving toward higher accuracy, the two relevant elements are the analogs of the real and virtual corrections

in a fixed-order calculation. We focus first on the real term, where we require the shower to generate the correct double-soft matrix element when two particles are produced at commensurate angles and (small) energies, while well-separated from all other particles.

Our approach is illustrated in Fig. 1. Consider the case where a dipole ab first emits a soft gluon $\tilde{1}$, followed by a splitting of the dipole $\tilde{1}b$ whereby a new particle 2 is emitted, and $\tilde{1}$ becomes 1 after recoil. When the branching from Eq. (1) produces a particle 2 from the $\tilde{1}b$ dipole, if $p_1 \cdot p_2 < p_2 \cdot p_b$, we select the $\{1, 2\}$ pair as the one whose double-soft effective matrix element needs correcting. To evaluate the double-soft correction to this configuration, we first identify all shower histories that could have produced the same nearby $\{1, 2\}$ pair. This includes the history actually followed by the shower, as well as the case where 2 was emitted from the $a\tilde{1}$ dipole, and two extra configurations where the shower produced a particle $\tilde{2}$ before 1, i.e., where, in the second splitting, gluon 1 was radiated with 2 taking the recoil.

Each history h is associated with an effective squared shower matrix element $|M_{\text{shower},h}|^2$, reflecting the probability that the shower, starting from the ab system, would produce the $\{1, 2\}$ pair in that order and color configuration (we address the question of the flavor configuration below). $|M_{\text{shower},h}|^2$ is evaluated in the double-soft limit; see Supplemental Material ([60], Sec. 2a). In principle, emission 2 should be accepted with probability

$$P_{\text{accept}} = \frac{|M_{\text{DS}}|^2}{\sum_h |M_{\text{shower},h}|^2}, \quad (3)$$

where $|M_{\text{DS}}|^2$ is the known double-soft matrix element for emitting the $\{1, 2\}$ soft pair from the ab dipole [62–64]. In practice, however, there are regions where the shower underestimates the true matrix element, leading to $P_{\text{accept}} > 1$. Nevertheless, we find that P_{accept} always remains smaller than some finite value Ω . We therefore enhance the splitting probability Eq. (2) by an overhead factor Ω , and accept the emission with probability P_{accept}/Ω .

The numerator and denominator in Eq. (3) are evaluated in the same double-soft limit, defined by rescaling $p_1 \rightarrow \lambda p_1$, $p_2 \rightarrow \lambda p_2$, and taking the limit $\lambda \rightarrow 0$. This ensures that $P_{\text{accept}} = 1$ when 1 and 2 are well-separated, thus not affecting regions where the shower was already correct.

The acceptance procedure is sufficient to ensure the proper generation of the $\{1, 2\}$ kinematics, but not the relative weights of the $a12b$ and $a21b$ color connections, which is crucial to reproduce the pattern of subsequent much softer radiation from the $\{a, 1, 2, b\}$ system, as required for NSL accuracy. To address this problem, we evaluate $F_{\text{shower}}^{(12)}$, the fraction of the shower effective double-soft matrix element associated with the $a12b$

color connection, and similarly $F_{\text{DS}}^{(12)}$ for the full double-soft matrix element, in its large- N_c limit [63,64]. If the shower has generated the $a12b$ color connection and $F_{\text{shower}}^{(12)} > F_{\text{DS}}^{(12)}$, then we swap the color connection with probability

$$P_{\text{swap}} = \frac{F_{\text{shower}}^{(12)} - F_{\text{DS}}^{(12)}}{F_{\text{shower}}^{(12)}}. \quad (4)$$

We apply a similar procedure when the shower generates the $a21b$ connection. In practice, we precede the color swap with an analogous procedure for adjusting the relative weights of gg and $q\bar{q}$ flavors for the $\{1, 2\}$ pair. An alternative would have been to apply P_{accept} separately for each color ordering and flavor combination. However, when we investigated that option for the PanGlobal class of showers, we encountered regions of phase space where the acceptance probability was unbounded. Illustrative plots of the shower matrix element and corrections are given in the Supplemental Material [60], Sec. 2b.

Next, we address the question of virtual corrections. When $\tilde{\Gamma}$ is produced in the deep soft-collinear region of the ab dipole, i.e., $\theta_{a\tilde{\Gamma}} \ll \theta_{ab}$ or $\theta_{b\tilde{\Gamma}} \ll \theta_{ab}$, the inclusion of K_{CMW} in Eq. (2) already accounts for second order contributions to the branching probability in the soft-collinear region, as required for NLL accuracy for global event shapes. However, in general, K_{CMW} alone is not sufficient when $\theta_{a1} \sim \theta_{1b} \sim \theta_{ab}$, notably because of the nontrivial $\tilde{\eta}$ dependence in Eq. (2) and the way in which it connects with the overall event momentum Q . Therefore, we need to generalize $K_{\text{CMW}} \rightarrow K(\Phi_{\tilde{\Gamma},ab})$, where the full K is a function of the kinematics of $\tilde{\Gamma}$ and of the opening angle of the ab dipole. In the same vein as the MC@NLO [65] and POWHEG [66,67] methods and their MINLO [68,69] extension, the correct next-to-leading order (NLO) normalization for the emission is given by

$$K(\Phi_{\tilde{\Gamma},ab}) = V(\Phi_{\tilde{\Gamma},ab}) + \int d\Phi_{12/\tilde{\Gamma}}^{\text{PS}} |M_{12/\tilde{\Gamma}}^{(\text{PS})}|^2 - \Delta_{\tilde{\Gamma}}^{(\text{PS},1)}. \quad (5)$$

Here, V is the exact QCD 1-loop contribution for a single soft emission, renormalized at scale $\mu = k_{t,\tilde{\Gamma}}$; $d\Phi_{12/\tilde{\Gamma}}^{\text{PS}} |M_{12/\tilde{\Gamma}}^{(\text{PS})}|^2$ is the product of shower phase space and matrix element associated with real $\tilde{\Gamma} \rightarrow 12$ branching, including double-soft corrections; and $\Delta_{\tilde{\Gamma}}^{(\text{PS},1)}$ is the coefficient of $\alpha_s/(2\pi)$ in the fixed-order expansion of the shower Sudakov factor. To aid in the evaluation of $K(\Phi_{\tilde{\Gamma},ab})$ we make use of two main elements: firstly, in the soft-collinear limit, $K(\Phi_{\tilde{\Gamma},ab}) \rightarrow K_{\text{CMW}}$; secondly, both $V(\Phi_{\tilde{\Gamma},ab})$ and $\Delta_{\tilde{\Gamma}}^{(\text{PS},1)}$ are independent of the rapidity of $\tilde{\Gamma}$, as long as $\tilde{\Gamma}$ is soft and (for $\Delta_{\tilde{\Gamma}}^{(\text{PS},1)}$) kept at some fixed value of

the evolution scale. We can therefore reformulate Eq. (5) as $K = K_{\text{CMW}} + \Delta K$, with

$$\Delta K = \int_r d\Phi_{12/\tilde{\Gamma}}^{(\text{PS})} |M_{12/\tilde{\Gamma}}^{(\text{PS})}|^2 - \int_{r_{\text{sc}}} d\Phi_{12/\tilde{\Gamma}_{\text{sc}}}^{(\text{PS})} |M_{12/\tilde{\Gamma}_{\text{sc}}}^{(\text{PS})}|^2. \quad (6)$$

In the second term, $\tilde{\Gamma}_{\text{sc}}$ is at the same shower scale v as $\tilde{\Gamma}$, but shifted by a constant in rapidity with respect to ab so as to be in the soft-collinear region, wherein $K(\Phi_{\tilde{\Gamma}_{\text{sc}},ab}) \rightarrow K_{\text{CMW}}$. The labels r and r_{sc} indicate a regularization of the phase space, which should be equivalent between the two terms. Specifically, we separate M_{DS} in Eq. (3) into correlated and uncorrelated parts, respectively those involving $C_F C_A$ versus C_F^2 color factors for the $\bar{q}ggq$ matrix element. For the correlated part, we cut on the relative transverse momentum of 1 and 2, while for the uncorrelated part, we cut on the transverse momentum with respect to the ab dipole and impose $|\Delta y_{12}| < \Delta y_{\text{max}}$. In practice we tabulate ΔK as a function of θ_{ab} , $\tilde{\eta}_{\tilde{\Gamma}}$, and $\phi_{\tilde{\Gamma}}$, though one could also envisage on-the-fly evaluation. We incorporate ΔK in Eq. (2), through a multiplicative factor $1 + \tanh[(\alpha_s/2\pi)\Delta K(1 - a_k)(1 - b_k)]$. This form keeps the correction positive and bounded. It also leaves the shower unmodified in the hard-collinear region.

We study the above approach with several variants of the PanGlobal shower. All have been adapted relative to Ref. [2] with regards to the precise way in which they restore momentum conservation after the map of Eq. (1). This was motivated by the discovery that in higher-order shower configurations involving three similarly collinear hard particles, the original recoil prescription could lead to unwanted long-distance kinematic side effects. Details are given in the Supplemental Material [60], Sec. 1, and tests were carried out using the method of Ref. [75].

We will consider three variants of the PanGlobal shower: two choices of the ordering variable, $\sim k_t \theta^\beta$ with $\beta = 0$ ($\text{PG}_{\beta=0}$) and $1/2$ ($\text{PG}_{\beta=1/2}$), and also a ‘‘split-dipole-frame’’ $\beta = 0$ variant ($\text{PG}_{\beta=0}^{\text{sdf}}$), which replaces $f(\pm\tilde{\eta}) \rightarrow f(\pm\eta)$ in Eq. (2), with $\eta = \frac{1}{2} \log a_k/b_k$. The $\eta = 0$ transition region bisects the dipole in its rest frame rather than the event frame. This makes the $\tilde{\Gamma} \rightarrow 12$ branching independent of the $\tilde{\Gamma}$ rapidity in the dipole frame, resulting in $\Delta K = 0$. Illustrative plots of ΔK and its impact are given in Ref. [60], Sec. 2c. For the three shower variants, the overhead factors Ω associated with Eq. (3) are respectively taken equal to 3.1, 20, and 4, independently of the dipole kinematics.

All results, both with and without double-soft corrections, include NLO 2-jet matching [70], which is required for the NN DL and NSL accuracy that we aim for. Spin correlations [71,72] are turned off because we have yet to integrate them with the double-soft corrections. The double-soft corrections are implemented at large N_c , in such a way as to preserve the full- N_c NLL and NDL accuracies

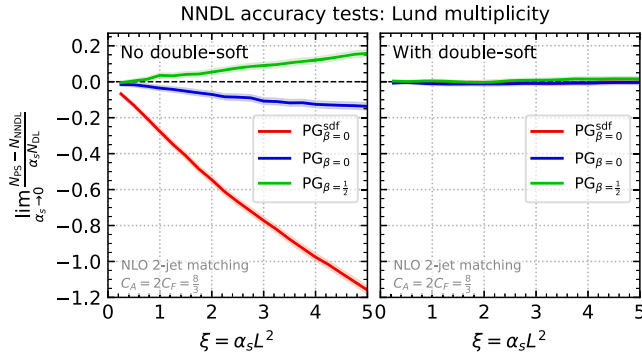


FIG. 2. The result of Eq. (7) for three variants of the PanGlobal shower without double-soft corrections (left) and with them (right). The latter are consistent with NNDL accuracy. The bands represent statistical errors in an $\alpha_s \rightarrow 0$ extrapolation based on four finite α_s values.

obtained in Ref. [73] for global observables and multiplicities. All events have (positive) unit weight.

To test the enhanced logarithmic accuracy of the shower, the first observable that we consider is the Lund subjet multiplicity [43] in $e^+e^- \rightarrow q\bar{q}$ events. This is a perturbatively calculable observable that is conceptually close to the experimentally important total charged-particle multiplicity. For a center-of-mass energy Q and a transverse momentum cutoff k_t , the subjet multiplicity has a double-logarithmic resummation structure $\alpha_s^n L^{2n}$ with $L = \ln k_t/Q$. The PanGlobal showers already reproduce terms up to NDL $\alpha_s^n L^{2n-1}$. The addition of the double-soft corrections and matching [70] is expected to bring NNDL accuracy, $\alpha_s^n L^{2n-2}$. To test this, in Fig. 2, we examine

$$\lim_{\alpha_s \rightarrow 0} \frac{N_{\text{PS}} - N_{\text{NNDL}}}{\alpha_s N_{\text{DL}}} \Big|_{\text{fixed } \alpha_s, L}, \quad (7)$$

where N_{PS} is the parton-shower result and N_{NNDL} (N_{DL}) is the known analytic NNDL (DL) result [43]. The $\alpha_s \rightarrow 0$ limit follows the procedure from earlier work [2]. Equation (7) is expected to be zero if the parton shower is NNDL accurate. The original showers, without double-soft corrections (left), clearly differ from each other and from zero, by up to $\sim 100\%$. With double-soft corrections turned on (right), all three PanGlobal variants are consistent with zero, i.e., with NNDL accuracy, to within $\sim 1\%$.

Next we turn to the study of nonglobal logarithms at leading color. These were recently calculated at NSL accuracy [45,46,48], $\alpha_s^n L^{n-1}$, and are available in the corresponding ‘‘Gnole’’ code [46]. We again consider e^+e^- events, and sum the transverse energies (E_t) of particles with $|y| < 1$, where y is the rapidity with respect to an axis determined by clustering the event to two jets with the Cambridge algorithm [74]. The fraction of events where the sum is below some $E_{t,\text{max}}$ is denoted by Σ and for

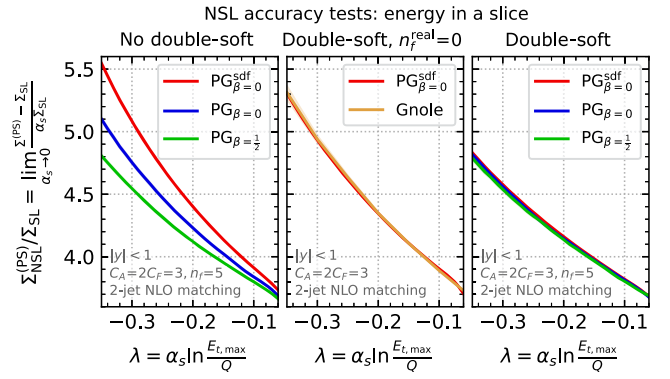


FIG. 3. Determinations of $\Sigma_{\text{NSL}}^{(\text{PS})}/\Sigma_{\text{SL}}$ for the transverse energy in a slice. Left: parton showers without double-soft corrections illustrating NSL differences between them. Middle: with double-soft corrections but $n_f^{\text{real}} = 0$ (cf. text for details), for comparison with the Gnole NSL code. Right: with full double-soft corrections, showing NSL agreement between the three PanGlobal showers.

a given shower we define

$$\Sigma_{\text{NSL}}^{(\text{PS})} = \lim_{\alpha_s \rightarrow 0} \frac{\Sigma^{(\text{PS})} - \Sigma_{\text{SL}}}{\alpha_s} \Big|_{\text{fixed } \alpha_s, L}, \quad L \equiv \ln \frac{E_{t,\text{max}}}{Q}. \quad (8)$$

Figure 3 (left) shows $\Sigma_{\text{NSL}}^{(\text{PS})}/\Sigma_{\text{SL}}$ for our three PanGlobal variants without double-soft corrections. As expected, they differ.

Figure 3 (middle) compares our $\text{PG}_{\beta=0}^{\text{sdf}}$ shower with double-soft corrections to the NSL Gnole code, showing good agreement, within $< 1\%$. Gnole has $n_f = 0$ in the real contribution and counterterm, but keeps the full $n_f = 5$ in the running of the coupling and inclusive K_{CMW} ($n_f^{\text{real}} = 0$). Among our showers it is relatively straightforward to make the same choice with $\text{PG}_{\beta=0}^{\text{sdf}}$, in particular because $\Delta K = 0$. Also, Gnole uses the thrust axis, while we use the jet axis; this is beyond NSL as the two axes coincide for hard three-parton events.

Figure 3 (right) shows the results from our three PanGlobal showers with complete (full- n_f) double-soft corrections included. They agree with each other to within 1% of the NSL contribution, providing a powerful test of the consistency of the full combination of the double-soft matrix element and ΔK across the variants. That plot also provides the first NSL calculation of nonglobal logarithms to include the full n_f dependence. An extended selection of results and comparisons is provided in Sec. 3 of Ref. [60].

We close with a brief examination of the phenomenological implications of the advances presented here. We consider $e^+e^- \rightarrow Z^* \rightarrow \text{jets}$ at $Q = 2$ TeV. This choice is intended to help gauge the size of nonglobal effects at the energies being probed today at the LHC. Figure 4 shows results for the distribution of energy flow in a rapidity slice, defined with respect to the 2-jet axis, without double-soft

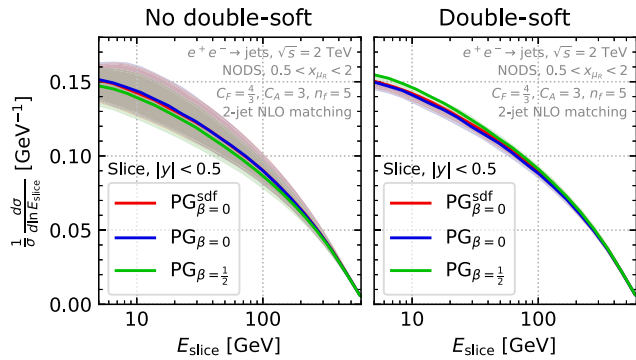


FIG. 4. Distribution of energy in a slice $|y| < 0.5$ for the PanGlobal shower without double-soft corrections (left) and with them (right). The bands represent renormalization scale variation, with NLO scale compensation enabled only for the results with double-soft corrections.

corrections (left) and with them, i.e., at NSL accuracy (right). It uses the nested ordered double-soft (NODS) color scheme, which while not full- N_c accurate for nonglobal logarithms, numerically coincides with the full- N_c single logarithmic results of Refs. [38–40], to within their percent-level numerical accuracy [73]. With a central scale choice (solid lines), the impact of the NSL corrections is modest. This is consistent with the observation from Fig. 3 that the NLL PanGlobal showers are numerically not so far from NSL accurate. However, the NSL double-soft corrections do bring a substantial reduction in the renormalization scale uncertainty, from about 10% to just a few percent. Conclusions are similar for $H^* \rightarrow gg$.

The results here provide the first demonstration that it is possible to augment parton-shower accuracy beyond NDJ and NLL. Specifically, our inclusion of real and virtual double-soft effects has simultaneously brought NNDL and NSL accuracy for two phenomenologically important classes of observable: multiplicities, and energy flows as relevant for isolation. It has also enabled the first leading-color, full- n_f predictions for NSL nonglobal logarithms. Overall, our methods and results represent a significant step toward a broader future goal of general next-to-next-to-leading logarithmic accuracy in parton showers.

We are grateful to Pier Monni for the very considerable work involved in the comparisons of NSL nonglobal logarithms for the energy flow in a slice, in particular with regards to the extraction of pure NSL results from the Gnole code. We are grateful to our PanScales collaborators (Melissa van Beekveld, Mrinal Dasgupta, Frédéric Dreyer, Basem El-Menoufi, Jack Helliwell, Rok Medves, Pier Monni, Alba Soto Ontoso, and Rob Verheyen), for their work on the code, the underlying philosophy of the approach, the adaptations of the PanGlobal shower discussed in Ref. [60], Sec. 1 and comments on this manuscript. This work has been funded by the European Research Council (ERC) under the European Union’s Horizon 2020

research and innovation program (Grant Agreements No. 788223, S.F.R., K.H., A.K., G.P.S., G.S., L.S.), by a Royal Society Research Professorship (RPR1\180112, G.P.S. and L.S.) and by the Science and Technology Facilities Council (STFC) under Grants No. ST/T000864/1 (G.P.S.) and No. ST/T000856/1 (K.H.). S.F.R., K.H., G.P.S., and L.S. benefited from the hospitality of the Munich Institute for Astro-, Particle and BioPhysics (MIAPbP), which is funded by the Deutsche Forschungsgemeinschaft (DFG, German Research Foundation) under Germany’s Excellence Strategy—EXC-2094—390783311. K.H., G.P.S., and L.S. also wish to thank CERN’s Theoretical Physics Department for hospitality while the work was being completed.

- [1] G. Bewick, S. Ferrario Ravasio, P. Richardson, and M. H. Seymour, *J. High Energy Phys.* **04** (2020) 019.
- [2] M. Dasgupta, F. A. Dreyer, K. Hamilton, P. F. Monni, G. P. Salam, and G. Soyez, *Phys. Rev. Lett.* **125**, 052002 (2020).
- [3] J. R. Forshaw, J. Holguin, and S. Plätzer, *J. High Energy Phys.* **09** (2020) 014.
- [4] Z. Nagy and D. E. Soper, *Phys. Rev. D* **104**, 054049 (2021).
- [5] Z. Nagy and D. E. Soper, [arXiv:2011.04777](https://arxiv.org/abs/2011.04777).
- [6] G. Bewick, S. Ferrario Ravasio, P. Richardson, and M. H. Seymour, *J. High Energy Phys.* **01** (2022) 026.
- [7] M. van Beekveld, S. Ferrario Ravasio, G. P. Salam, A. Soto-Ontoso, G. Soyez, and R. Verheyen, *J. High Energy Phys.* **11** (2022) 019.
- [8] M. van Beekveld, S. Ferrario Ravasio, K. Hamilton, G. P. Salam, A. Soto-Ontoso, G. Soyez, and R. Verheyen, *J. High Energy Phys.* **11** (2022) 020.
- [9] F. Herren, S. Höche, F. Krauss, D. Reichelt, and M. Schoenherr, [arXiv:2208.06057](https://arxiv.org/abs/2208.06057).
- [10] M. van Beekveld and S. Ferrario Ravasio, [arXiv:2305.08645](https://arxiv.org/abs/2305.08645).
- [11] B. Andersson, G. Gustafson, L. Lonnblad, and U. Petterson, *Z. Phys. C* **43**, 625 (1989).
- [12] F. A. Dreyer, G. P. Salam, and G. Soyez, *J. High Energy Phys.* **12** (2018) 064.
- [13] S. Catani, Y. L. Dokshitzer, M. Olsson, G. Turnock, and B. R. Webber, *Phys. Lett. B* **269**, 432 (1991).
- [14] S. Catani, Y. L. Dokshitzer, F. Fiorani, and B. R. Webber, *Nucl. Phys.* **B377**, 445 (1992).
- [15] S. Catani, B. R. Webber, Y. L. Dokshitzer, and F. Fiorani, *Nucl. Phys.* **B383**, 419 (1992).
- [16] M. Dasgupta and G. Salam, *Phys. Lett. B* **512**, 323 (2001).
- [17] M. Dasgupta and G. P. Salam, *J. High Energy Phys.* **03** (2002) 017.
- [18] A. Banfi, G. Marchesini, and G. Smye, *J. High Energy Phys.* **08** (2002) 006.
- [19] H. Weigert, *Nucl. Phys.* **B685**, 321 (2004).
- [20] Y. Hatta, *J. High Energy Phys.* **11** (2008) 057.
- [21] S. Caron-Huot, *J. High Energy Phys.* **03** (2018) 036.
- [22] J. Forshaw, J. Keates, and S. Marzani, *J. High Energy Phys.* **07** (2009) 023.
- [23] R. M. Duran Delgado, J. R. Forshaw, S. Marzani, and M. H. Seymour, *J. High Energy Phys.* **08** (2011) 157.

- [24] M. D. Schwartz and H. X. Zhu, *Phys. Rev. D* **90**, 065004 (2014).
- [25] T. Becher, M. Neubert, L. Rothen, and D. Y. Shao, *Phys. Rev. Lett.* **116**, 192001 (2016).
- [26] A. J. Larkoski, I. Moulton, and D. Neill, *J. High Energy Phys.* **09** (2015) 143.
- [27] T. Becher, M. Neubert, L. Rothen, and D. Y. Shao, *J. High Energy Phys.* **11** (2016) 019; **05** (2017) 154(E).
- [28] T. Becher, B. D. Pecjak, and D. Y. Shao, *J. High Energy Phys.* **12** (2016) 018.
- [29] D. Neill, *J. High Energy Phys.* **01** (2017) 109.
- [30] S. Caron-Huot and M. Herranen, *J. High Energy Phys.* **02** (2018) 058.
- [31] A. J. Larkoski, I. Moulton, and D. Neill, *J. High Energy Phys.* **11** (2016) 089.
- [32] T. Becher, R. Rahn, and D. Y. Shao, *J. High Energy Phys.* **10** (2017) 030.
- [33] R. Ángeles Martínez, M. De Angelis, J. R. Forshaw, S. Plätzer, and M. H. Seymour, *J. High Energy Phys.* **05** (2018) 044.
- [34] M. Balsiger, T. Becher, and D. Y. Shao, *J. High Energy Phys.* **08** (2018) 104.
- [35] D. Neill, *J. High Energy Phys.* **02** (2019) 114.
- [36] M. Balsiger, T. Becher, and D. Y. Shao, *J. High Energy Phys.* **04** (2019) 020.
- [37] M. Balsiger, T. Becher, and A. Ferroglia, *J. High Energy Phys.* **09** (2020) 029.
- [38] Y. Hatta and T. Ueda, *Nucl. Phys.* **B874**, 808 (2013).
- [39] Y. Hagiwara, Y. Hatta, and T. Ueda, *Phys. Lett. B* **756**, 254 (2016).
- [40] Y. Hatta and T. Ueda, *Nucl. Phys.* **B962**, 115273 (2021).
- [41] J. R. Forshaw, A. Kyrieleis, and M. H. Seymour, *J. High Energy Phys.* **08** (2006) 059.
- [42] J. R. Forshaw, A. Kyrieleis, and M. H. Seymour, *J. High Energy Phys.* **09** (2008) 128.
- [43] R. Medves, A. Soto-Ontoso, and G. Soyez, *J. High Energy Phys.* **10** (2022) 156.
- [44] R. Medves, A. Soto-Ontoso, and G. Soyez, *J. High Energy Phys.* **04** (2023) 104.
- [45] A. Banfi, F. A. Dreyer, and P. F. Monni, *J. High Energy Phys.* **10** (2021) 006.
- [46] A. Banfi, F. A. Dreyer, and P. F. Monni, *J. High Energy Phys.* **03** (2022) 135.
- [47] T. Becher, T. Rauh, and X. Xu, *J. High Energy Phys.* **08** (2022) 134.
- [48] T. Becher, N. Schalch, and X. Xu, [arXiv:2307.02283](https://arxiv.org/abs/2307.02283).
- [49] S. Jadach, A. Kusina, M. Skrzypek, and M. Slawska, *J. High Energy Phys.* **08** (2011) 012.
- [50] L. Hartgring, E. Laenen, and P. Skands, *J. High Energy Phys.* **10** (2013) 127.
- [51] S. Jadach, A. Kusina, W. Placzek, and M. Skrzypek, *Acta Phys. Pol. B* **44**, 2179 (2013).
- [52] S. Jadach, A. Kusina, W. Placzek, and M. Skrzypek, *J. High Energy Phys.* **08** (2016) 092.
- [53] H. T. Li and P. Skands, *Phys. Lett. B* **771**, 59 (2017).
- [54] S. Höche and S. Prestel, *Phys. Rev. D* **96**, 074017 (2017).
- [55] S. Höche, F. Krauss, and S. Prestel, *J. High Energy Phys.* **10** (2017) 093.
- [56] F. Dulat, S. Hoche, and S. Prestel, *Phys. Rev. D* **98**, 074013 (2018).
- [57] J. M. Campbell, S. Höche, H. T. Li, C. T. Preuss, and P. Skands, *Phys. Lett. B* **836**, 137614 (2023).
- [58] L. Gellersen, S. Höche, and S. Prestel, *Phys. Rev. D* **105**, 114012 (2022).
- [59] G. Gustafson and U. Pettersson, *Nucl. Phys.* **B306**, 746 (1988).
- [60] See Supplemental Material at <http://link.aps.org/supplemental/10.1103/PhysRevLett.131.161906> for further technical details.
- [61] S. Catani, B. R. Webber, and G. Marchesini, *Nucl. Phys.* **B349**, 635 (1991).
- [62] Y. L. Dokshitzer, G. Marchesini, and G. Oriani, *Nucl. Phys.* **B387**, 675 (1992).
- [63] J. M. Campbell and E. W. N. Glover, *Nucl. Phys.* **B527**, 264 (1998).
- [64] S. Catani and M. Grazzini, *Nucl. Phys.* **B570**, 287 (2000).
- [65] S. Frixione and B. R. Webber, *J. High Energy Phys.* **06** (2002) 029.
- [66] P. Nason, *J. High Energy Phys.* **11** (2004) 040.
- [67] S. Frixione, P. Nason, and C. Oleari, *J. High Energy Phys.* **11** (2007) 070.
- [68] K. Hamilton, P. Nason, and G. Zanderighi, *J. High Energy Phys.* **10** (2012) 155.
- [69] K. Hamilton, P. Nason, C. Oleari, and G. Zanderighi, *J. High Energy Phys.* **05** (2013) 082.
- [75] F. Caola, R. Grabarczyk, M. L. Hutt, G. P. Salam, L. Scyboz, and J. Thaler, [arXiv:2306.07314](https://arxiv.org/abs/2306.07314).
- [70] K. Hamilton, A. Karlberg, G. P. Salam, L. Scyboz, and R. Verheyen, *J. High Energy Phys.* **03** (2023) 224.
- [71] A. Karlberg, G. P. Salam, L. Scyboz, and R. Verheyen, *Eur. Phys. J. C* **81**, 681 (2021).
- [72] K. Hamilton, A. Karlberg, G. P. Salam, L. Scyboz, and R. Verheyen, *J. High Energy Phys.* **03** (2022) 193.
- [73] K. Hamilton, R. Medves, G. P. Salam, L. Scyboz, and G. Soyez, *J. High Energy Phys.* **03** (2021) 041.
- [74] Y. L. Dokshitzer, G. D. Leder, S. Moretti, and B. R. Webber, *J. High Energy Phys.* **08** (1997) 001.